264 *Journal of Electrical Engineering & Technology Vol. 7, No. 2, pp. 264~272, 2012*
http://dx.doi.org/10.5370/JEET.2012.7.2.264

Medical Image Compression Using Quincunx Wavelets and SPIHT Coding

M. Beladgham†, A. Bessaid*, A. Taleb-Ahmed and I. Boucli Hacene***

Abstract – In the field of medical diagnostics, interested parties have resorted increasingly to medical imaging. It is well established that the accuracy and completeness of diagnosis are initially connected with the image quality, but the quality of the image is itself dependent on a number of factors including primarily the processing that an image must undergo to enhance its quality. This paper introduces an algorithm for medical image compression based on the quincunx wavelets coupled with SPIHT coding algorithm, of which we applied the lattice structure to improve the wavelet transform shortcomings. In order to enhance the compression by our algorithm, we have compared the results obtained with those of other methods containing wavelet transforms. For this reason, we evaluated two parameters known for their calculation speed. The first parameter is the PSNR; the second is MSSIM (structural similarity) to measure the quality of compressed image. The results are very satisfactory regarding compression ratio, and the computation time and quality of the compressed image compared to those of traditional methods.

Keywords: Medical image, Compression, Quincunx wavelets, Lattice, SPIHT

1. Introduction

The massive use of numerical methods in medical imaging (MRI, X scanner, nuclear medicine, etc.…) today generates increasingly important volumes of data. The problem becomes even more critical with the generalisation of 3D sequence. So it is necessary to use compressed images in order to limit the amount of data to be stored and transmitted.

Among many compression schemes by transformation have been proposed, we can cite the standards JPEG images, MPEG 1 and 2 for compressing video. All of these standards are based on the discrete cosine transform (DCT) [1].

Over the past ten years, the wavelets (DWT), have had a huge success in the field of image processing, and have been used to solve many problems such as image compression and restoration [2]. However, despite the success of wavelets in various fields of image processing such as encoding, weaknesses have been noted in its use in the detection and representation of the objects' contours. The wavelets transform and other classical multi resolutions decompositions seem to form a restricted and limited class of opportunities for multi-scale represen-tations of multidimensional signals.

To overcome this problem, we propose a new multi resolution decompositions by quincunx wavelets which are better adapted to the image representation.

† Corresponding Author: Faculty of Sciences and Technology, Bechar University, Algeria. (beladgham@yahoo.fr)
* Biomedical Engineering laboratory, Tlemcen University, Algeria
** Biomecanic Laboratory, University of Valencienne, France
Received: June 18, 2010; Accepted: December 27, 2011

This structure of decomposition allows the construction of a nonseparable transform. Nonseparable wavelets, by contrast, offer more freedom and can be better tuned to the characteristics of images. Their less attractive side is that they require more computations. The quincunx wavelets are especially interesting because they are nearly isotropic [3]. In contrast with the separable case, there is a single wavelet and the scale reduction is more progressive: one factor instead of 2.

2. Quincunx Wavelets

The separable dyadic analysis require three families of wavelets, which is sometimes regarded as a disadvantage, in addition the factor of addition between two successive scales is 4 which may seem high. It is possible to solve these two problems, but at the cost of the loss of filter separability and therefore a slightly higher computational complexity. An analysis has been particularly well studied to find a practical application, known as "quincunx" [1]. Quincunx decomposition results in fewer subbands than most other wavelet decompositions, a feature that may lead to reconstructed images with slightly lower visual quality. The method is not used much in practice, but [4] presents results that suggest that quincunx decomposition performs extremely well and may be the best performer in many practical situations. Fig. 1 illustrates this type of decomposition. [3]

We notice that the dilation factor is not more than 2 between two successive resolutions, and that only one wavelet family is necessary [5, 6]. In this case the

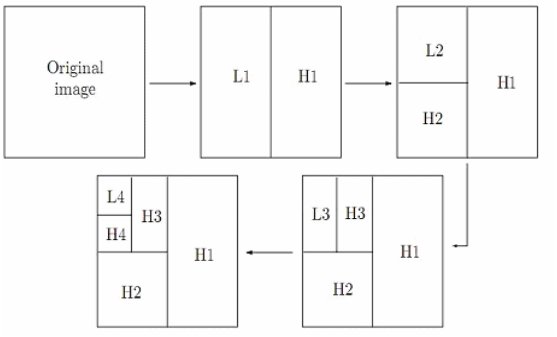

Fig. 1. Quincunx wavelet decomposition

dilatation matrix will be:

$$M=\begin{bmatrix}1 & 1\\ 1 & -1\end{bmatrix}$$

The Grid transformation (lattice) is done according to $y_{i+1}[\vec{n}]$ the following diagram:

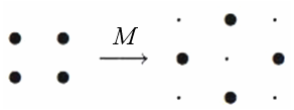

This matrix generates a quincunx lattice in 2D. The column vectors of this matrix form a basis to this lattice. The volume of the unit cell associated equals 2. The same lattice (Fig. 2) is also emanating from the matrix below [1]

$$M'=\begin{bmatrix}1 & -1\\ 1 & 1\end{bmatrix}$$

It is noticed that the dilatation step is $\sqrt{2}$ on each direction and the geometry of the grid obtained justifies the name given to this multiresolution analysis.

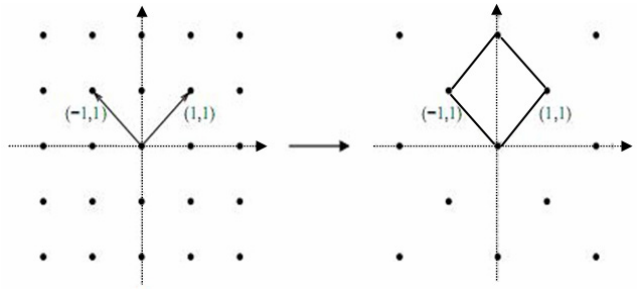

(a) Lattice quincunx (b) Unit cell

Fig. 2. Examples of a lattice quincunx and unit cell

3. Quincunx Sampling and Filter banks

First, we recall some basic results on quincunx sampling and perfect reconstruction filterbanks [7, 8]. The quincunx sampling lattice is shown in Fig. 3. Let $x[\vec{n}]$ with $\vec{n}=(n_1,n_2)\in Z^2$ denote the discrete signal on the initial grid. The two-dimensional (2-D) z-transform of $x[\vec{n}]$ is denoted by:

$$X(\vec{z})=\sum_{\vec{n}\in Z^2} x[\vec{n}]\vec{z}^{-\vec{n}}\text{, where } \vec{z}^{\vec{n}}=\vec{z}^{n_1}\,\vec{z}^{n_2} \qquad (1)$$

The continuous 2-D Fourier transform is then given by $X(e^{j\vec{\omega}})=\sum_{\vec{n}\in Z^2} x[\vec{n}]e^{-j(\vec{\omega},\vec{n})}$ with $\vec{\omega}=(\omega_1,\omega_2)$ and, finally, the discrete 2-D Fourier transform for $x[\vec{n}]$ given on an N x N grid $(n_1,n_2 = 0,1,...,N-1)$ by

$$X[\vec{k}]=\sum_{\vec{n}\in Z^2} x[\vec{n}]e^{-j2\pi(\vec{k},\vec{n})/N},$$
with $(k_1,k_2 = 0,1,...,N-1)$.

Now, we write the quincunx sampled version of $x[\vec{n}]$ as:

$$[x]_{\downarrow M}[\vec{n}] = x[M\,\vec{n}] \quad where \quad M=\begin{pmatrix}1 & 1\\ 1 & -1\end{pmatrix} \qquad (2)$$

Our down-sampling matrix M is such that $M^2 = 2I$. where I is identity matrix.

The Fourier domain version of (2) is

$$[x]_{\downarrow M}[\vec{n}] \leftrightarrow \frac{1}{2}\left[X(e^{jM^{-T}\vec{\omega}})+X(e^{j(M^{-T}\vec{\omega}+\vec{\pi})})\right] \qquad (3)$$

where $\vec{\pi}=(\pi,\pi)$.

The up-sampling is defined by

$$[x]_{\uparrow M}[\vec{n}]=\begin{cases}x[M^{-1}\vec{n}], & when\ n_1+n_2\ is\ even\\ 0 & elsewhere\end{cases} \qquad (4)$$

and its effect in the Fourier domain is as follows:

$$[x]_{\uparrow M}[\vec{n}] \longleftrightarrow X(e^{jM^T\vec{\omega}}) \qquad (5)$$

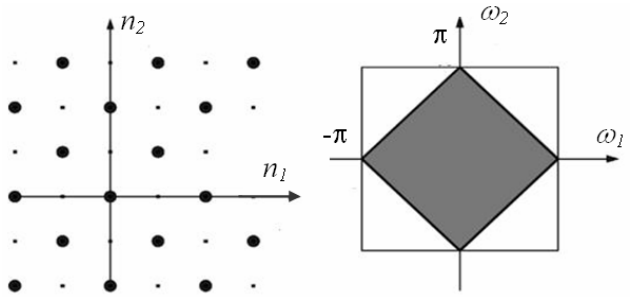

(a) (b)

Fig. 3. (a) Quincunx lattice; (b) the corresponding Nyquist area in the frequency domain

If we now chain the down-sampling and up-sampling operators, we get

$$[x]_{\downarrow M\uparrow M}[\vec{n}]=\begin{cases}x[\vec{n}], & when\ \ n_1+n_2\ \ is\ \ even\\ 0 & elsewhere\end{cases} \tag{6}$$

$$[x]_{\downarrow M\uparrow M}[\vec{n}]=\frac{1}{2}\left[X(e^{j\vec{\omega}})+X(e^{j(\vec{\omega}+\vec{\pi})})\right] \tag{7}$$

Since quincunx sampling reduces the number of image samples by a factor of two, the corresponding reconstruction filterbank has two channels (Fig. 4). The low-pass filter $\tilde{H}$ reduces the resolution by a factor of $\sqrt{2}$; the wavelet coefficients correspond to the output of the high-pass filter $\tilde{G}$. [8-10].

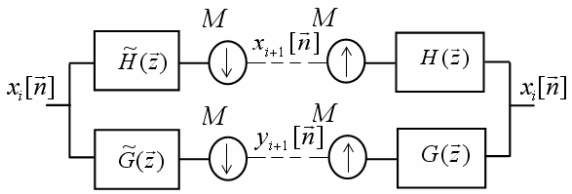

Fig. 4. Perfect reconstruction filter bank on a quincunx lattice

Applying the relation (7) to the block diagram in Fig. 4, it is easy to derive the conditions for a perfect reconstruction

$$\begin{cases}\tilde{H}(\vec{z})H(\vec{z})+\tilde{G}(\vec{z})G(\vec{z})=2\\ \tilde{H}(-\vec{z})H(\vec{z})+\tilde{G}(-\vec{z})G(\vec{z})=0\end{cases} \tag{8}$$

Where H and G (respectively $\tilde{H}$ and $\tilde{G}$) are the transfer functions of the synthesis (respectively analysis) filters. In the orthogonal case, the analysis and synthesis filters are identical up to a central symmetry; the wavelet filter G is simply a modulated version of the low-pass filter H.

4. Fractional Quincunx Filters

To generate quincunx filters, we will use the standard approach which is to apply the diamond McClellan transform to map a 1-D design onto the quincunx structure. [11]

4.1 New 1-D wavelet family

As starting point for our construction, we introduce a new 1-D family of orthogonal filters

$$H_\alpha(z)=\frac{\sqrt{2}\,(z+2+z^{-1})^{\frac{\alpha}{2}}}{\sqrt{(z+2+z^{-1})^{\alpha}+(-z+2-z^{-1})^{\alpha}}} \tag{9}$$

$$H_\alpha(\omega)=\frac{\sqrt{2}\,(2+2\cos\omega)^{\frac{\alpha}{2}}}{\sqrt{(2+2\cos\omega)^{\alpha}+(2-2\cos\omega)^{\alpha}}} \tag{10}$$

which is indexed by the continuously-varying order parameter α.

These filters are symmetric and are designed to have zeros of order α at $z=-1$; the numerator is a fractional power of $(z+2+z^{-1})$ (the simplest symmetric refinement filter of order 2) and the denominator is the appropriate L2-orthonormalization factor. Also note that these filters are maximally flat at the origin; they essentially behave $H_\alpha(z)/\sqrt{2}=1+O(\omega^\alpha)$ as $\omega\to 0$. Their frequency response is similar to the Daubechies' filters with two important differences: 1) the filters are symmetric and 2) the order is not restricted to integer values. [8, 9]

4.2 Corresponding 2-D wavelet family

Applying the diamond McClellan transform to the filter above is straightforward; it amounts to replacing $\cos\omega$ by $(1/2)(\cos\omega_1+\cos\omega_2)$ in (10). Thus, our quincunx refinement filter is given by

$$H_\alpha(e^{j\vec{\omega}})=\frac{\sqrt{2}\,(2+\cos\omega_1+\cos\omega_2)^{\frac{\alpha}{2}}}{\sqrt{(2+\cos\omega_1+\cos\omega_2)^{\alpha}+(2-\cos\omega_1-\cos\omega_2)^{\alpha}}} \tag{11}$$

This filter is guaranteed to be orthogonal because the McClellan transform has the property of preserving biorthogonality. Also, by construction, the α th order zero at $\omega=\pi$ gets mapped into a corresponding zero at $(\omega_1,\omega_2)=(\pi,\pi)$; this is precisely the condition that is required to get a 2-D wavelet transform of order α. Also, note the isotropic behavior and the flatness of $H_\alpha(e^{j\vec{\omega}})$ around the origin; i.e, $H_\alpha(e^{j\vec{\omega}})/\sqrt{2}=1+O(\|\vec{\omega}\|^\alpha)$ for $\vec{\omega}\to 0$. The orthogonal wavelet filter is obtained by modulation

$$G_\alpha(\vec{z})=z_1H_\alpha(-\vec{z}^{-1}) \tag{12}$$

The corresponding orthogonal scaling function is defined implicitly as the solution of the quincunx two-scale relation

$$\varphi_\alpha(\vec{x})=\sqrt{2}\sum_{\vec{n}\in Z^2}h_\alpha[\vec{n}]\varphi_\alpha(M\vec{x}-\vec{n}) \tag{13}$$

Since the refinement filter is orthogonal with respect to the quincunx lattice, it follows that $\varphi_\alpha(\vec{x})\in L_2(R^2)$ and that it is orthogonal to its integer translates. Moreover, for $\alpha>0$, it will satisfy the partition of unity condition, which comes as a direct consequence of the vanishing of the filter

at $(\omega_1,\omega_2)=(\pi,\pi)$ Thus, we have the guarantee that our scheme will yield orthogonal wavelet bases of $L_2(R^2)$. The underlying orthogonal quincunx wavelet is simply

$$\psi_\alpha(\vec{x})=\sqrt{2}\sum_{\vec{n}\in Z^2} g_\alpha[\vec{n}]\varphi_\alpha(M\vec{x}-\vec{n}) \quad (14)$$

5. SPIHT Coding Scheme

When the decomposition image is obtained, we try to find a way how to code the wavelet coefficients into an efficient result, taking redundancy and storage space into consideration. The Set Partitioning in Hierarchical Trees (SPIHT) [12, 13] is one of the most advanced schemes available, even outperforming the state-of-the-art JPEG 2000 in some situations. The basic principle is the same; a progressive coding is applied, processing the image respectively to a lowering threshold. The difference is in the concept of zerotrees (spatial orientation trees in SPIHT). This is an idea that takes bounds between coefficients across subbands in different levels into consideration [13]. The first idea is always the same: if there is an coefficient in the highest level of transform in a particular subband considered insignificant against a particular threshold, it is very probable that its descendants in lower levels will be insignificant too, so we can code quite a large group of coefficients with one symbol. Fig. 5 shows how a spatial orientation tree is defined in a pyramid constructed with recursive six iterations splitting. The coefficients are ordered in hierarchies. According to this relationship, the SPIHT algorithm saves many bits that specify insignificant coefficients [14].

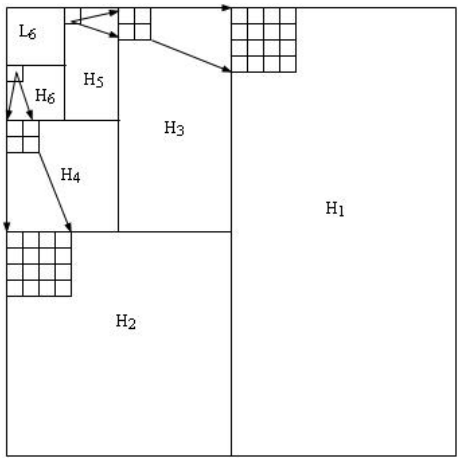

Fig. 5. Parent-child relationship

The flowchart of SPIHT is presented in Fig. 6. First step, the original image is decomposed into subbands. Then the method finds the maximum and the iteration number. Second step, the method puts the quincunx wavelets coefficients into sorting pass that finds the significance coefficients in all coefficients and encodes the sign of these significance coefficients. Third step, the significance coefficients that be found in sorting pass are put into the refinement pass that use two bits to exact the reconstruct value for closing to real value.

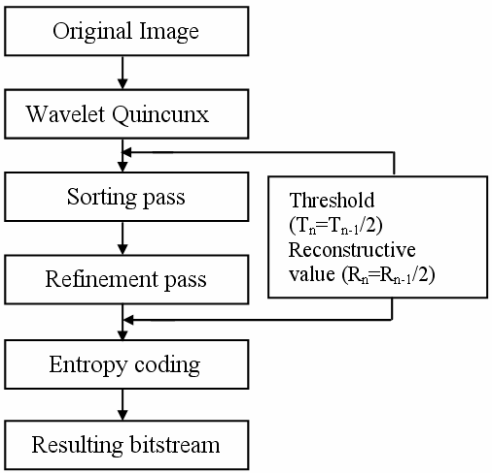

Fig. 6. Flowchart of SPIHT

The front second and third steps are iterative, next iteration decreases the threshold ($T_n=T_{n-1}/2$) and the reconstructive value ($R_n=R_{n-1}/2$). Forth step, the encoding bits access entropy coding and then transmit [15]. The result is in the form of a bitstream. The quincunx wavelet-based-image encoding algorithms improve the compression rate and the visual quality.

6. Compression Quality Evaluation

The Peak Signal to Noise Ratio (PSNR) is the most commonly used as a measure of quality of reconstruction in image compression. The PSNR were identified using the following formulate:

$$MSE = \frac{1}{M\,x\,N}\sum_{1=1}^{i=M}\sum_{j=1}^{j=N}\left(I(i,j) - \hat{I}(i,j)\right)^2 \quad (15)$$

Mean Square Error (MSE) which requires two *M*x*N* grayscale images I and $\hat{I}$ where one of the images is considered as a compression of the other is defined as:

• The PSNR is defined as:

$$PSNR = 10\log_{10}\left(\frac{(Dynamics\quad of\quad image)^2}{MSE}\right) \quad (16)$$

Usually an image is encoded on 8 bits. It is represented by 256 gray levels, which vary between 0 and 255, the extent or dynamics of the image is 255.

• The structural similarity index (SSIM):

The PSNR measurement gives a numerical value on the damage, but it does not describe its type. Moreover, as is often noted in [16, 17], it does not quite represent the quality perceived by human observers. For medical imaging applications where images are degraded must eventually be examined by experts, traditional evaluation remains insufficient. For this reason, objective approaches are needed to assess the medical imaging quality. We then evaluate a new paradigm to estimate the quality of medical images, specifically the ones compressed by wavelet transform, based on the assumption that the human visual system (HVS) is highly adapted to extract structural information. The similarity compares the brightness, contrast and structure between each pair of vectors, where the structural similarity index (SSIM) between two signals x and y is given by the following expression [18, 19]:

$$SSIM\ (x,y)=l(x,y).c(x,y).s(x,y) \tag{17}$$

However:

- The comparison of brightness is determined by the following expression:

$$l(x,y)=\frac{2\mu_x\,\mu_y+C_1}{\mu_x+\mu_y+C_1} \tag{18}$$

Where

The average intensity of signal x is given by: $\mu_x=\frac{1}{N}\sum_{i=1}^{N}x_i$

$C_1=(K_1\,L)^2$, the constant $K_1<<1$ and L: the dynamic row of the pixel values (255 for an image in gray scale coded on 8 bits).

- The function of contrast comparison takes the following form:

$$c(x,y)=\frac{2\sigma_x\,\sigma_y}{\sigma_x^2+\sigma_y^2+C_2} \tag{19}$$

where

$\sigma_x=\sqrt{\mu_x(x^2)-\mu_x^2}$: The standard deviation of the original signal x.

$C_2=(K_2\,L)^2$, the constant $K_2<<1$

- The function of structure comparison is defined as follows:

$$s(x,y)=\frac{\sigma_{xy}+C_3}{\sigma_x\,\sigma_y+C_3}=\frac{\mathrm{cov}\ (x,y)+C_3}{\sigma_x\,\sigma_y+C_3} \tag{20}$$

where

$\mathrm{cov}\ (x,y)=\mu_{xy}-\mu_x\,\mu_y$, $C_3=\frac{C_2}{2}$

Then the expression of the structural similarity index becomes:

$$SSIM\ \ (x,y)=\frac{(2\mu_x\,\mu_y+C_1)(2\sigma_{xy}+C_2)}{(\mu_x^2+\mu_y^2+C_1)(\sigma_x^2\,\sigma_y^2+C_2)} \tag{21}$$

Finally the quality measurement can provide a spatial map of the local image quality, which provides more information on the image quality degradation, which is useful in medical imaging applications. For application, we require a single overall measurement of the whole image quality that is given by the following formula:

$$MSSIM\ (I,\hat{I})=\frac{1}{M}\sum_{i=1}^{M}SSIM\ (I_i,\hat{I}_i) \tag{22}$$

Where I and $\hat{I}$ are respectively the reference and degraded images, I_i and $\hat{I}_i$ are the contents of images at the i-th local window.

M : the total number of local windows in image. The MSSIM values exhibit greater consistency with the visual quality.

7. Results and Discussion

We are interested in lossy compression methods based on 2D wavelet transforms because of their interesting properties. Indeed, the 2D wavelet transforms combines good spatial and frequency locations. As we work on medical image, the spatial location and frequency are important [20, 21].

In this article we have applied our algorithm to compress medical images. For this reason we have chosen an axial slice of human brain size 512x512 (grayscale), encoded on 8 bits per pixel, and recorded by means of an MRI scanner. This image is taken from the GE Medical System database [22].

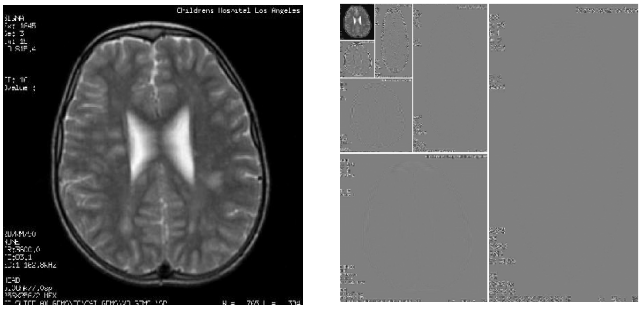

(a) Axial slice (b) Quincunx wavelet decomposition

Fig. 7. Original image

The importance of our work lies in the possibility of reducing the rates for which the image quality remains acceptable. Estimates and judgments of the compressed image quality is given by the PSNR evaluation parameters and the MSSIM similarity Index.

Fig. 8 shown below illustrates the compressed image quality for different bit-rate values (number of bits per pixel). According to the PSNR and MSSIM values, we note that from 0.5bpp, image reconstruction becomes almost perfect.

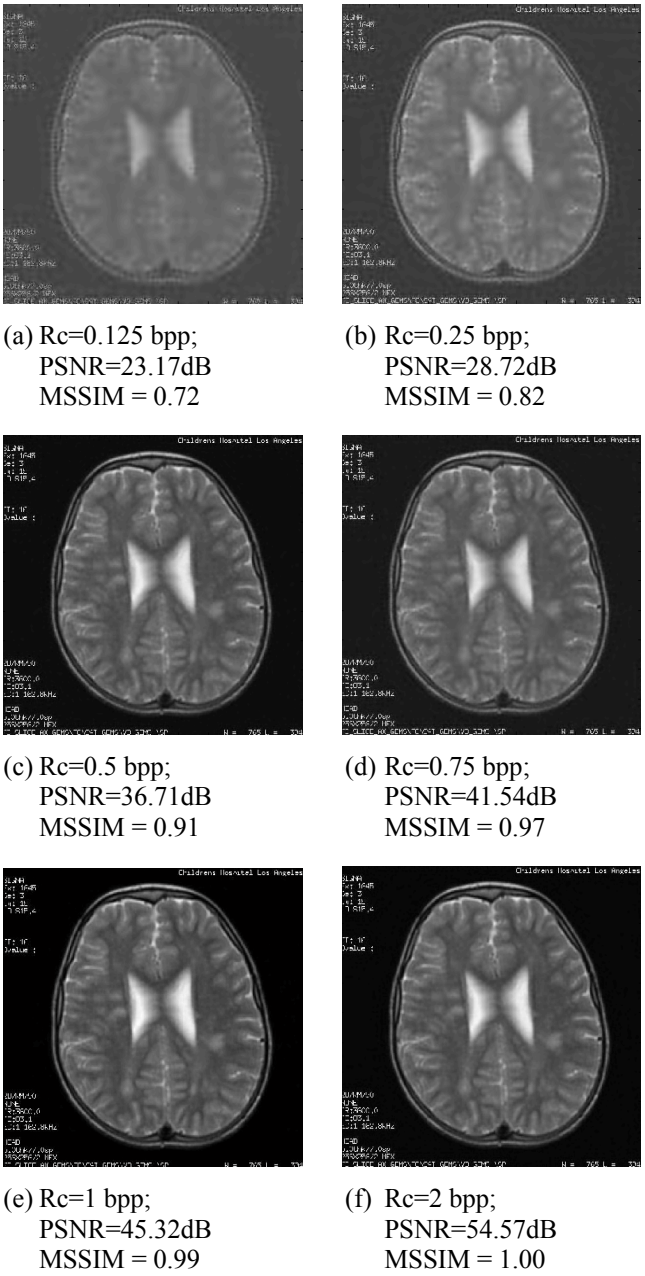

(a) Rc=0.125 bpp; PSNR=23.17dB MSSIM = 0.72

(b) Rc=0.25 bpp; PSNR=28.72dB MSSIM = 0.82

(c) Rc=0.5 bpp; PSNR=36.71dB MSSIM = 0.91

(d) Rc=0.75 bpp; PSNR=41.54dB MSSIM = 0.97

(e) Rc=1 bpp; PSNR=45.32dB MSSIM = 0.99

(f) Rc=2 bpp; PSNR=54.57dB MSSIM = 1.00

Fig. 8. Compressing of an axial slice with Quincunx wavelet and SPIHT coding

To show the performance of the proposed method, we will now make a comparison between these different types of transform (Quincunx wavelet; CDF 9/7 (Filter Bank) and CDF9/7 (Lifting scheme)) coupled with the SPIHT coding and CDF9/7 (Lifting scheme) combined with the EZW coding. For each application we vary the bit-rate 0.125 to 2 and calculate the PSNR and MSSIM. The results obtained are given in Table 1.

Table 1. PSNR and MSSIM variation using different methods (Axial slice)

R_c (bpp)	Quincunx wavelet + SPIHT		CDF9/7 (Lifting) + SPIHT	
	PSNR	MSSIM	PSNR	MSSIM
0.125	23.17	0.72	19.79	0.59
0.25	28.72	0.82	25.74	0.76
0.5	36.71	0.91	34.95	0.91
0.75	41.54	0.97	40.74	0.97
1	45.32	0.99	45.03	0.99
1.5	50.39	0.99	50.76	1.00
2	54.57	1.00	55.17	1.00

R_c (bpp)	CDF9/7(Filter bank) + SPIHT		CDF9/7 (Lifting) + EZW	
	PSNR	MSSIM	PSNR	MSSIM
0.125	18.38	0.59	19.44	0.58
0.25	23.62	0.63	22.65	0.70
0.5	32.22	0.80	29.85	0.82
0.75	37.88	0.89	34.61	0.90
1	42.32	0.95	37.93	0.94
1.5	48.07	0.98	43.27	0.98
2	52.19	0.99	46.77	0.99

The comparison in terms of image quality for the four algorithms is given by the PSNR and MSSIM curves represented in Figs. 9 and 10.

Comparing the different values of PSNR and MSSIM, we show clearly the efficiency of our algorithm in terms of compressed image quality for the low bit-rate.

This study was subsequently generalized to a set of medical images of the GE Medical Systems database. The following figure (Fig. 11) presents the results obtained after application of different algorithms on an axial slice of body imaging. These results are obtained with a 0.5-bpp bit-rate.

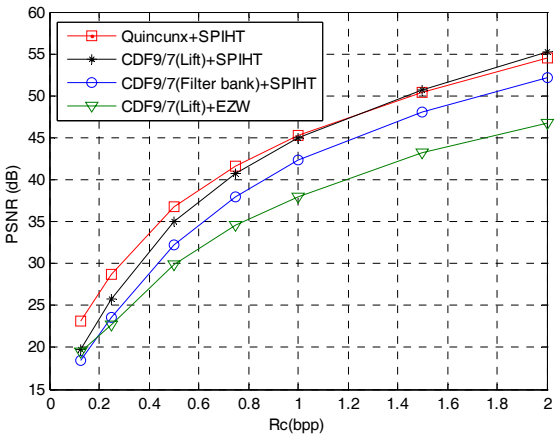

Fig. 9. PSNR variation using different methods

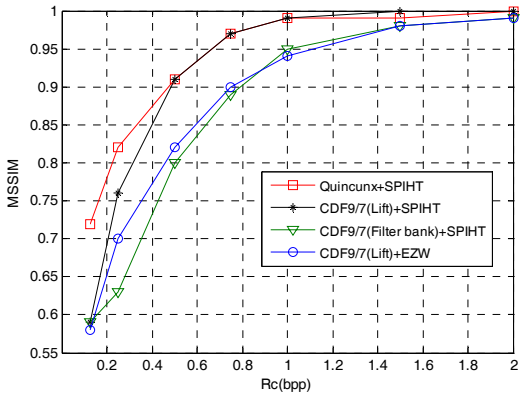

Fig. 10. MSSIM variation using different methods

Original Image

Quincunx wavelet +SPIHT
Rc=0. 5 bpp;
PSNR=35.99dB
MSSIM = 0.93

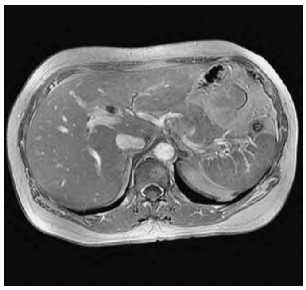

CDF9/7 (Lifting sheme)
+SPIHT
Rc=0. 5 bpp;
PSNR=35.43 dB
MSSIM = 0.92

CDF9/7 (Filter Bank)
+SPIHT
Rc=0. 5 bpp;
PSNR=32. 81 dB
MSSIM = 0.85

CDF9/7 (Lifting sheme)
+EZW
Rc=0. 5 bpp;
PSNR=30.93 dB
MSSIM = 0.85

Fig. 11. Compressing of an axial slice of Body imaging

The following figures (Fig. 12, Fig. 13) present a set of medical images (MRI) from GE Healthcare database [23], compressed by the quincunx wavelets algorithm for a 0.5-bpp bit-rate.

We can say that our compression algorithm better preserves the different image structures for bit-rates higher or equal to 0.5 bpp.

Patient - Male
Age - 52 years
Exam performed with CTL coil
Sag FRFSE-XL T2 4mm
Patient in serious aggravation
Plaque of demyelinization, multiple sclerosis

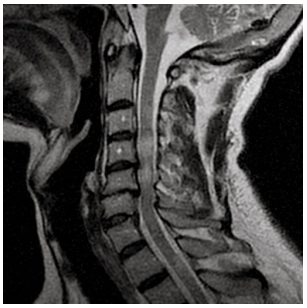

Original Image

Quincunx wavelet +SPIHT
Rc=0. 5 bpp;
PSNR=37.24 dB
MSSIM = 0. 93

Fig. 12. Neuro imaging

Patient - Female
Age - 45 years
Intra-articular effusion
Exam acquired with the Head coil.
Sag T2 GRE 3mm

Original Image

Quincunx wavelet +SPIHT
Rc=0. 5 bpp;
PSNR=41.96 dB
MSSIM = 0. 97

Fig. 13. Orthopedic imaging

8. Conclusion

The objective of this paper is undoubtedly the enhancement of medical images quality after the compression step. The latter is regarded as an essential tool to aid diagnosis (storage or transmission) in medical imaging. We used the quincunx wavelet compression coupled with the SPIHT coding. After several applications, we found that this algorithm gives better results than the other compression techniques.

To develop our algorithm, we used various types of medical images. We have noticed that for 0.5 bpp bit-rate, the algorithm provides very important PSNR and MSSIM values for MRI images. Thus, we conclude that the results obtained are very satisfactory in terms of compression ratio and compressed image quality.

In perspective, we aspire to apply our algorithm to compress video sequences.

References

[1] Chappelier V., "Progressive coding of images by directed wavelet", *Phd. Thesis*, Rennes1 University, December 15th ,2005.

[2] Mallat S., "Multifrequency channel decompositions of images and wavelet models", *IEEE Transaction in Acoustic Speech and Signal Processing*, Vol. 37, pp. 2091-2110, Dec. 1989

[3] Salomon D. "Data ompression", *The Complete Reference*,Third Edition, Springer.

[4] Stromme, Oyvind. "On The Applicability of Wavelet Transforms to Image and Video Compression", *Ph.D. thesis*, University of Strathclyde, February 1999.

[5] Truchetet F. "Wavelets for digital signal", *Hermes Edition,* Paris, January 1998.

[6] Tanaka Y., Ikehara M and Truong Q. N , "A New Combination of 1D and 2D Filter Banks for Effective Multiresolution Image Representation" ; *IEEE*, pp 2820-2823, 2008.

[7] Vetterli M. and Kovacevé J., "Wavelets and Subband Coding", *Upper Saddle River*, NJ: Prentice-Hall, 1995.

[8] Manuela F., Dimitri VD. and Michael U., "An Orthogonal Family of Quincunx Wavelets With Continuously Adjustable Order", *IEEE Transactions On Image Processing*, Vol. 14, No. 4, APRIL 2005.

[9] Dimitri VD., Thierry B. and Michael U. "On the Multidimensional Extension of the Quincunx Subsampling Matrix", *IEEE Signal Processing Letters*, Vol. 12, No. 2, FEBRUARY 2005.

[10] Chen Y. Michael AD. and Wu-Sheng L. "Design of Optimal Quincunx Filter Banks for Image Coding", *EURASIP Journal on Advances in Signal Processing*, Vol. 2007.

[11] Lee L., Oppenheir V.A., "Proprerties of approximate parks-McClellan filters", *IEEE*, pp.2165-2168; 1997;

[12] Miaou S.G., Chen S.T. and Chao S.N., "Wavelet-based lossy-to-lossless medical image compression using dynamic VQ and SPIHTcoding", *Biomedical engineering-applications, basis & communications*, Vol. 15 No3, p 235-242, December 2003.

[13] Said A. and Pearlman W. A., "A new fast and efficient image codec based on set partitioning in hierarchical trees", *IEEE Trans. Circuits and Systems for Video Technology*, Vol. 6, p243 – 250, June 1996.

[14] Yen-Yu C. and Shen-Chuan T., "Embedded medical image compression Using DCT based subband decomposition and modified SPIHT data organization", *Proceedings of the Fourth IEEE*, (BIBE'04), 2004.

[15] Xiong Z., Ramchandran K., and Orchard M., "Space-frequency quantization for wavelet image coding", *IEEE Trans. Image Processing*, Vol. 6, No. 5, pp 677–693, May 1997.

[16] Geisler W. S. and Banks M. S., "Visual performance", *in Handbook of Optics* (M. Bass, ed.), McGraw-Hill, 1995.

[17] Watson A. B. and Kreslake L., "Measurement of visual impairment scales for digital video", *in Human Vision, Visual Processing, and Digital Display, Proc. SPIE*, Vol. 4299, 2001.

[18] Wang Z., Bovik A. C., Sheikh H. R. and Simoncelli E.P, "Image quality assessment: From error visibility to structural similarity", *IEEE Transactions on Image Processing*, Vol. 13, No. 4, APRIL 2004.

[19] Wang Z. and Bovik A. C, "A universal image quality index", *IEEE Signal Processing Letters*, Vol. 9, pp.81–84, Mar. 2002.

[20] Buccigrossi R. W. and Simoncelli E. P., "Image compression via joint statistical characterization in the wavelet domain", *IEEE Trans. Image processing,* Vol. 8, pp. 1688–1701, December 1999.

[21] Chandler D. M. and Hemami S. S., "Additivity models for suprathreshold distortion in quantized wavelet-coded images", *in Human Vision and Electronic Imaging VII, Proc. SPIE*, Vol. 4662, Jan. 2002.

[22] www.GE Medical System.com (database).

[23] www. GE Healthcare.com (database).

Mohammed BELADGHAM obtained the Engineer degree in Electronics from university of Tlemcen, Algeria, and then a Magister in signals and systems from university of Tlemcen, Algeria. His research interests are Image processing, Medical image compression, wavelets transform and optimal encoder.

Abdelhafid BESSAID was born in Tlemcen, Algeria. He received the dipl. El.-Ing. degree from the University of Sciences and Technology of Oran (USTO, Algeria); the Master degree and the PHD from the University of Sidi Bel Abbes (Algeria), respectively in 1981, 1991 and 2004. He Works, since 1996, in the field of Medical Imaging and Image Processing at University of Tlemcen, Algeria.

Abdelmalik TALEB-AHMED was born in Roubaix, France, in 1962. He received a post graduate degree and a Ph. D. in Electronics and Microwaves from the University of Lille1 in 1988 and 1992. From 1992 to 2004, He was an Associate Professor at the University of Littoral, Calais. Since 2004, He is currently a Professor at the University of Valenciennes in the department GE2I, and does his research at the LAMIH FRE CNRS 3304 UVHC, His research interests includes signal and image processing. Image segmentation, Prior knowledge integration in image analysis, Partial Differential Equations and Variational Methods in image analysis, Image compression, Multimodal signal processing, Medical image analysis, including multimodal image registration, etc.

Ismail BOUKLI HACENE obtained the Engineer degree in Electronics from university of Tlemcen, Algeria, and then a Magister in Electronic Biomedical from university of Tlemcen, Algeria. His research interests are Image processing, Medical image compression, wavelets transform and optimal encoder.